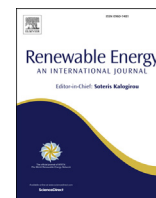


### **4.3 Paper III: Wind over complex terrain - microscale modelling with two types of mesoscale winds at Nygårdsfjell**



# Wind over complex terrain – Microscale modelling with two types of mesoscale winds at Nygårdstjell



Muhammad Bilal <sup>a, \*</sup>, Yngve Birkelund <sup>a</sup>, Matthew Homola <sup>b</sup>, Muhammad Shakeel Virk <sup>c</sup>

<sup>a</sup> The Arctic University of Norway, Norway

<sup>b</sup> Nordkraft AS, Norway

<sup>c</sup> Narvik University College, Norway

## ARTICLE INFO

### Article history:

Received 23 December 2015

Received in revised form

3 June 2016

Accepted 17 July 2016

### 2010 MSC:

00–01

99–00

### Keywords:

Wind speed

Complex terrain

Meso-scale modelling

Micro-scale modelling

WRF

## ABSTRACT

Nygårdstjell, a complex terrain near Norwegian-Swedish border, is characterized by its significant wind resources. The feasibility of using mesoscale winds as input to microscale model is studied in this work. The main objective is to take into account the actual terrain effects on wind flow over complex terrain. First set of mesoscale winds are modelled with Weather Research and Forecasting (WRF) numerical tool whereas second set of mesoscale winds are taken from the Modern-Era Retrospective Analysis for Research and Applications (MERRA) data system. WindSim, a computational fluid dynamics based numerical solver is used as microscale modelling tool. The results suggest that the performance of microscale model is largely dependent upon the quality of mesoscale winds as input. The proposed coupled models achieve improvements in wind speed modelling, especially during cold weather. WRF-WindSim coupling showed better results than MERRA-WindSim coupling in all three test cases, as root mean square error (RMSE) decreased by 70.9% for the February case, 61.5% for October and 14.4% for June case respectively. Raw mesoscale winds from the WRF model were also more correct than the mesoscale winds from MERRA data set when extracted directly at the wind turbine by decreasing the RMSE by 62.6% for the February case, 62.7% for October and 23.7% for June case respectively. The difference of RMSE values between the mesoscale winds directly at wind turbine versus the coupled meso-microscale model outputs are not conclusive enough to indicate any specific trend.

© 2016 The Authors. Published by Elsevier Ltd. This is an open access article under the CC BY-NC-ND license (<http://creativecommons.org/licenses/by-nc-nd/4.0/>).

## 1. Introduction

The most critical factor in wind farm performance is the wind speed itself. Consequently, the accurate prediction of wind speed is a key research field for the industry as well as the academics. Until recently, meteorological institutes all over the world have undertaken wind prediction research. However, due to rapid expansion in wind farm industry and its introduction into conventional grid, there is a need to build a bridge between the meteorological researches regarding the wind speed prediction and its direct application into wind industry.

Meteorological models have proven themselves very useful in predicting various environmental variables, mostly because they are equipped with the possibility of wide range of configurations. This diversity also poses a challenge to find the right set of

configurations and the numerical and physical schemes that are also dependent on the multidimensional and nonlinear interactions [1]. The first and the foremost challenge is to find the correct combination of configurations of the model to use in a specific area. Having said that, the best configuration for one area might well not be suitable to other areas [2]. Changes in the configuration of these models provide understanding of how the models react to it and how it effects their output. It also narrows down the most sensitive parameters to the model [3] [4].

Meteorological models are not good to resolve physical processes on all scales and the atmospheric processes can occur in range of  $10^{-2}$  meters to  $10^8$  meters spatially and  $10^{-1}$  seconds to  $10^8$  seconds temporally [5]. So unresolved physical processes are handle by physical parameterization schemes. However, the down side of using these schemes is that these parameterization schemes are based on assumptions and approximations so in the event of these assumptions and approximations going wrong results in introducing errors in the model [6]. Topography also plays a crucial role on the climate of the region. Orographic features may

\* Corresponding author.

E-mail address: [muhammad.bilal@uit.no](mailto:muhammad.bilal@uit.no) (M. Bilal).

substantially affect the regional climate by influencing the dynamics of the atmospheric circulation and the interaction between the atmosphere and the land [7] [8]. On a micro scale, the local terrain plays a vital role influencing the surrounding atmospheric circulation. Increasing the resolution of simulation domain will make it possible for the model to capture the complex terrain effects on wind flow. However, the improvement in results may not justify the high computational costs [9].

The Nygårdsfjell wind farm is located in a valley at approximately 420 m above sea level surrounded by mountains in the north and south near the Norwegian-Swedish border. Majority of the winds are suspected to be originating from Torneträsk lake in east which is covered with ice during the winter time. The air closest to the surface on surrounding mountains gets colder and denser. The air then slides down the hill and accumulates over the lake. The air then spills out westward towards Ofotfjord through the broader channel that directs and transforms it into speeding winds. Previous study at Nygårdsfjell wind farm indicated high wind events particularly during the winters. These events consist of wind speeds between 12 and 24 m/s and one of them lasted up to four and a half days uninterruptedly. Majority of these high winds are coming from East of the wind farm [10].

In this study, an attempt is made to couple two types of meso-scale winds with computational fluid dynamics (CFD) based microscale model to better estimate the wind circulations over the complex terrain at Nygårdsfjell wind farm. The method is expected to provide better understanding of wind flow over complex terrain of Nygårdsfjell. The quality of input mesoscale winds are expected to have direct influence on microscale model output. The mesoscale winds are taken from WRF and MERRA, whereas WindSim is used as microscale model. This is not the preferred method of meso-microscale model coupling, but this method is evaluated as it was expected to be easier to implement and to check if it could still give valuable results. The proposed method is applied to three selected cases due to resource constraints. The cases are taken from the previous research work at the Nygårdsfjell wind farm [10]. The objective was to model high wind events over different seasons. The intention of the work is to introduce a potentially promising method that is recommended to be tested on larger data sets. Measured data is compared with the coupled model output in terms of RMSE.

The outline of the paper is as follows: Description of the data set is given in section 2. Section 3 explains the model configurations and simulation setup of WRF and WindSim followed by Section 4 discussing various coupling methods of mesoscale winds with microscale model. Results are discussed in section 5, whereas conclusion is made in section 6.

## 2. Data sets

Primarily two types of mesoscale winds are used as input to WindSim model. First set of mesoscale winds are generated by WRF simulations. The data is generated by setting up WRF simulations centered around the Nygårdsfjell wind farm as explained in section 3.

The second set of mesoscale winds are taken from the Modern-Era Retrospective Analysis for Research and Applications (MERRA), provided by NASA [11–13]. MERRA reanalysis data reconstruct the atmospheric state by integrating data from different sources such as conventional and satellite data [14]. MERRA uses a three-dimensional variational (3d-Var) analysis algorithm based on the Grid-point Statistical Interpolation scheme [15]. It provides worldwide grid of wind data at a spatial resolution of  $1/2^\circ$  latitude and  $2/3^\circ$  longitude that translates to approximately  $27 \text{ km} \times 57 \text{ km}$  grid size with hourly temporal resolution since 1979. The wind data

is based on the northward and eastward wind components at three different heights (2, 10 and 50 m) above ground level (a.g.l) that can be utilized to obtain the wind speed and the corresponding direction at the hub height. The focus of the research is not to carry out a detail technical evaluation of the data generating strategy of MERRA but rather focus on the usage of MERRA data in the wind energy industry. In-depth details are provided in Ref. [15,16]. In this research work, MERRA dataset is extracted at the nearest available point for its use in microscale modelling.

Measured dataset is taken from three 2.3 MW Siemens wind turbines (SWT-2.3-93) with hub height of 80 m that were installed at Nygårdsfjell during the fall of 2005. The data is filtered and analyzed for the high wind events and three test cases are selected in June 2008, October 2008 and February 2009.

## 3. Model setup

WRF model is run at the super computing facility of Texas Tech University, USA whereas WindSim simulations are done in collaboration with Narvik University College. The author followed the user manual of the WindSim for setting up the model and running the simulations. The model configurations are given in the following.

### 3.1. WRF

One set of mesoscale winds are generated by running the WRF model at the Nygårdsfjell wind farm. WRF version 3.5.1 of the Advanced Research (ARW) solver which is a widely used meso-scale model developed by the National Center for Atmospheric Research (NCAR) is used. It is a successor to NCAR Fifth-Generation meso-scale Model (MM5). WRF offers multiple physics options that can be combined in different ways. The options typically range from simple and efficient to sophisticated and more computationally costly and from newly developed schemes to the well-trying schemes. WRF has a wide set of physical parameterization schemes available for micro physics, radiation (long wave and short wave), cumulus and related to the boundary layer: surface layer, planetary boundary layer (PBL) and land surface model. Physical parameterization schemes interact non-linearly with each other and with the dynamical core of the model, and these complex relationships make the interpretation of model deficiencies very challenging.

For current analysis, mesoscale winds from the WRF model are generated by using the PBL scheme; local closure turbulent kinetic energy scheme Mellor-Yamada-Janjic along with the short/long wave radiation scheme Goddard. The selected PBL settings may not be optimal for this site, but are similar to previous settings that have been used with success in other research work [17–19]. The initial and boundary conditions supplied to the WRF model were taken from the ERA-Interim data sets from the European Center for Medium-Range Weather Forecasts, with spectral resolution of approximately 80 km on 60 vertical levels with 6 h of temporal sampling. Land use and topographical properties are acquired from the US Geological Survey. The simulation domains are shown in Fig. 1. The parent domain (d01) has a spatial resolution of  $18 \times 18 \text{ km}$ , covering most of the north Norway. The inner nested domains (d02 and d03) have spatial resolutions of  $6 \times 6 \text{ km}$  and  $2 \times 2 \text{ km}$  respectively. The vertical resolution of the model consists of 51 levels. All domains are centered around the wind turbine location: Latitude =  $68^\circ 30' 27''$ ; Longitude =  $17^\circ 87' 27''$ . Interaction protocol feedback from nest to its parent domain is selected. All the results discussed in this paper lie within the inner most domain that is d03 and are converted to hourly temporal resolution to be consistent with other models.

### WPS Domain Configuration

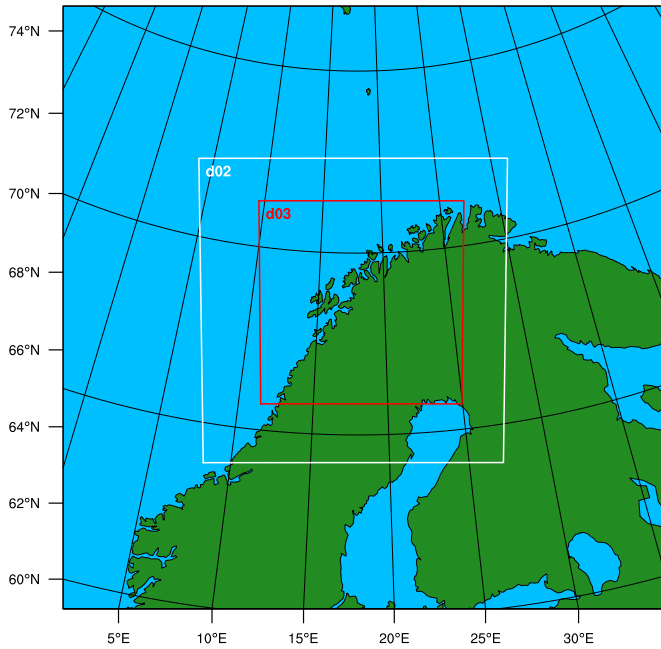
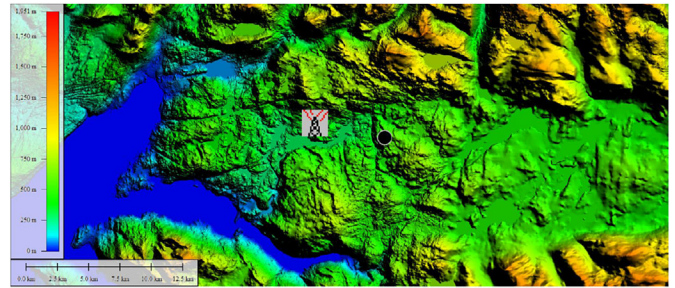
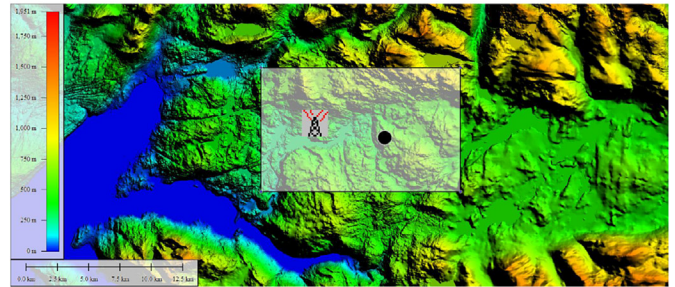


Fig. 1. WRF – Simulation domains.



(a) General terrain of the area



(b) WindSim domain

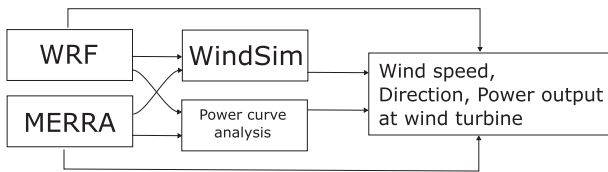
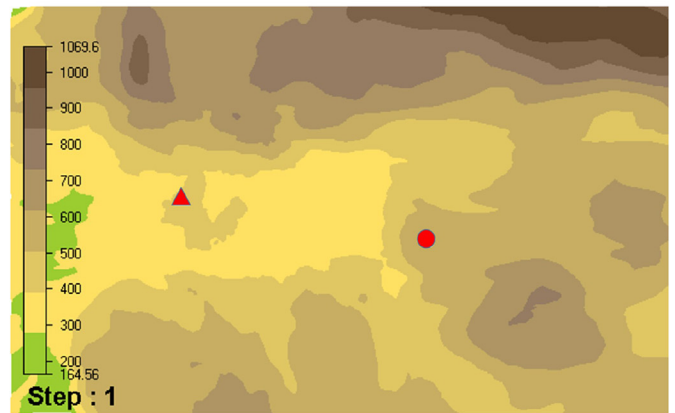


Fig. 2. Flow diagram.

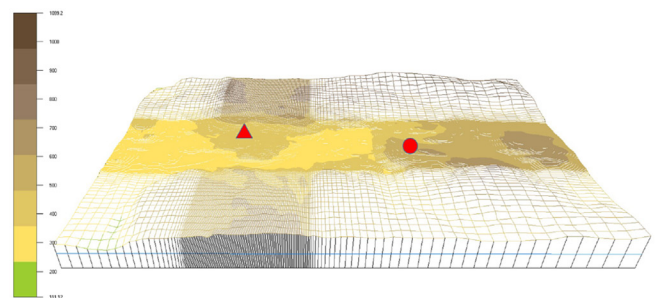
### 3.2. WindSim

WindSim uses the general collocated velocity method to solve the flow equations in body-fitted geometries. The solver is based on the Reynolds Averaged Navier-Stokes equations. The model solves the atmospheric flow for a steady-state case for a chosen wind direction. The model is run for a given set of constructed boundary and initial conditions. The standard k-e turbulence closure scheme is applied in WindSim [20]. For our simulations, the boundary and initial conditions used are: no nesting, number of sectors 12, height of boundary layer 500 m, speed above boundary layer height 10 m per second, and at the top of boundary layer fixed pressure condition is used. The digital terrain model has spatial resolution of 20 m × 20 m. The output data has hourly temporal resolution for coherent analysis with other models.

Fig. 3 shows the digital terrain model of Nygårdsfjell wind farm, which was imported into WindSim. Fig. 3 (a) describes the overall location (approx. 50 km × 25 km) around the wind farm with wind turbine marked as tower and virtual climatology point as circle. The white box in (b) describes the area domain (x-min:612800.000, x-max:628700.000 and y-min:7597300.000, y-max:7607200.000 – Universal Transverse Mercator meters) in WindSim. The area includes mountains on North and South sides and extends to relatively lower altitude areas on East and West with minimum elevation of 110.7 m a.g.l, maximum of 1107.5 m a.g.l and average of 550 m a.g.l. The area represents an ideal test case for wind over complex terrain with maximum slope of 74.63° and average slopes



(c) WindSim terrain model



(d) WindSim multimesh terrain model

Fig. 3. Site location.

of 11°. Fig. 3 (C) shows the terrain model of the area domain in WindSim and (d) shows the refined multi-mesh including the wind

turbine and climatology points within it. The grid extends 6865 m a.g.l above the point in the terrain with the highest elevation in WindSim. The grid is refined towards the ground.

#### 4. Analysis of various coupling methods

Coupling mesoscale winds with microscale model means that the output of a mesoscale model should be used as the input to a microscale model. There are many outputs and inputs for these models, which means that there are many variations on how to couple the models. In addition to the choice of parameters, wind speed, temperature, heat flux and so on, there must also be a choice of location (X,Y, and Z), one or multiple locations, and how to handle a difference in grid scale for a chosen location.

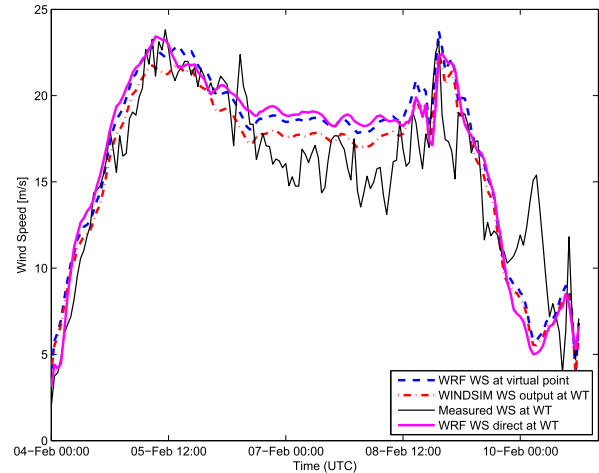
In this study, mesoscale winds are coupled into microscale model through virtual climatology. This means that the wind speed and direction at a specific location (X,Y,Z) are extracted from the mesoscale model and used as input at the same location (X,Y,Z) in the microscale model. All other parameters in the microscale model are fixed as described in section 3.2. This is not the preferred method of meso-microscale model coupling, but this method is evaluated as it was expected to be easier to implement and to check if it could still give valuable results. In order to avoid the interpolation losses, the closest available MERRA data point in East (Latitude = 68° 30' 00'; Longitude = 18° 00' 00') is selected as a virtual climatology. In terms of horizontal resolution of input mesoscale winds, the WRF values at this grid point represent an area average over 2 km × 2 km, whereas MERRA dataset value represent an area average of 27 km × 57 km. In terms of vertical resolution, WRF values at 80 m are used and MERRA dataset values only available at 50 m therefore 50 m is used. This is done to avoid the general under/over predictions of wind speeds by going higher/lower levels in altitudes [20–23]. No systematic differences were found in outputs by changing the mesoscale winds input altitudes in WindSim. Furthermore real power curve of installed wind turbine is used with the mesoscale winds from WRF and MERRA directly at the wind turbine to estimate the power output. Fig. 2 summarizes the methodology.

### 5. Results and discussion

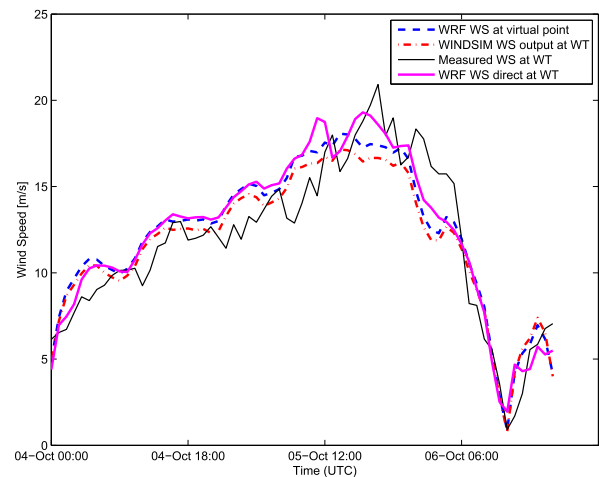
#### 5.1. Wind speed analysis

Figs. 4 and 5 show the result of wind speed outputs from the two coupled models. Fig. 4 shows the WRF wind speed at the virtual point (the coupling point between WRF and Windsim), the WRF-WindSim coupled model wind speed (WINDSIM WS output at WT) at the wind turbine, the measured wind speed at the wind turbine, and the WRF wind speed extracted directly at the wind turbine location. For all three cases, it can be seen that the WRF model catches the major ramp up and down changes in wind speed, the exception being the spike in wind speed near the end of case (a) which was not captured by the model. For case (a), it can be seen that the couple WRF-WindSim model seems to better match the dip in wind speed in the middle portion of the event. The amplitude of the events matches well for the cases (a) and (b), but for the case (c) there is an underestimation of the wind speed even though the shape of the curves are similar to the measured wind speeds. As reported in another study, one of the potential reasons of underperforming WRF model in summer is the failure of the selected PBL scheme to capture the terrain induced thermal circulations that are common in mountainous region during warmer seasons [24].

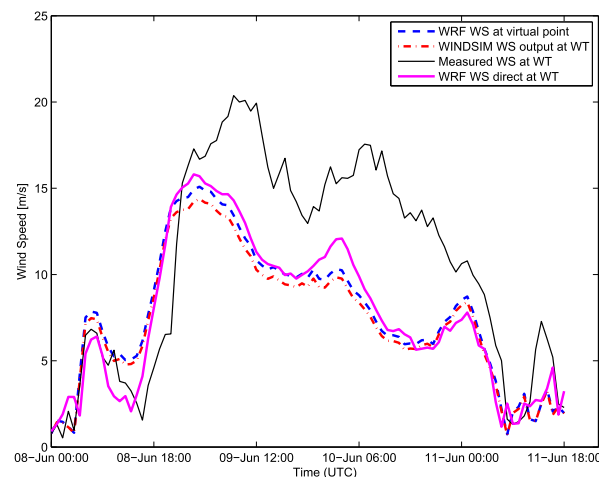
Fig. 5 shows the MERRA wind speed at the virtual point (coupling point between MERRA and Windsim), the MERRA-WindSim coupled model wind speed (WINDSIM WS output at



(a) Case: February 4-10 2009

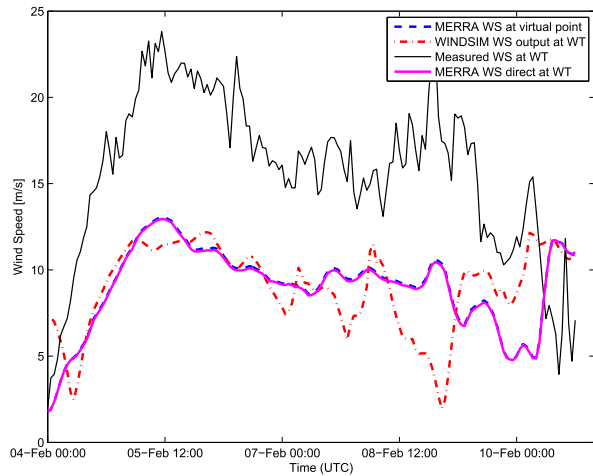


(b) Case: October 4-6 2008

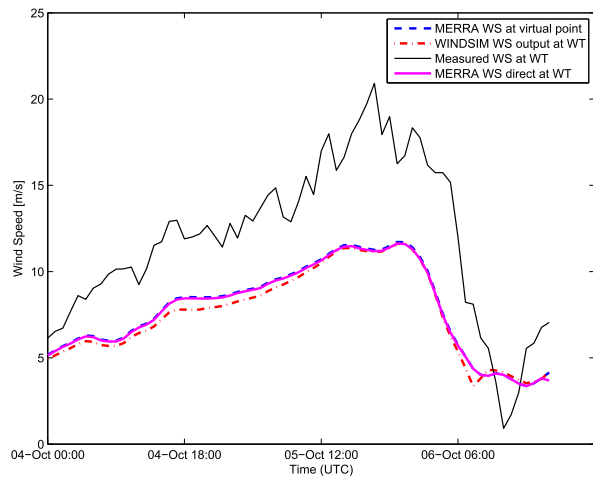


(c) Case: June 8-11 2008

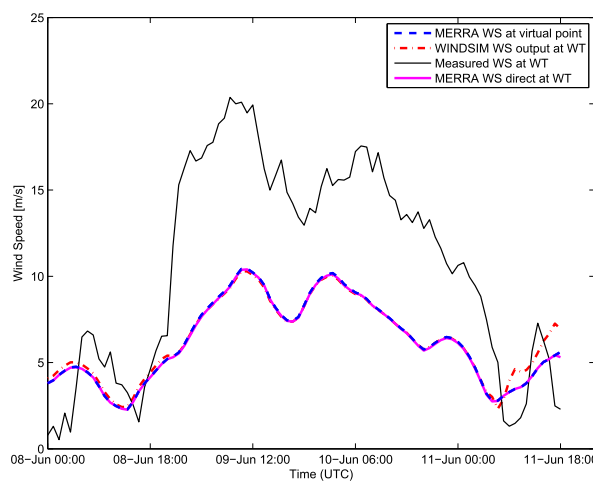
Fig. 4. Comparison of WRF, WindSim WS output vs measured values.



(a) Case: February 4-10 2009



(b) Case: October 4-6 2008



(c) Case: June 8-11 2008

Fig. 5. Comparison of MERRA, WindSim WS output vs measured values.

WT) at the wind turbine, the measured wind speed at the wind turbine, and the MERRA wind speed extracted directly at the wind turbine location. For all three cases, there is an underestimation of the wind speed even though the shape of the curves are similar to the measured wind speeds. The exception being the turbulent pattern in case (a). The amplitudes of the events do not matches well for all the cases (a), (b), and (c).

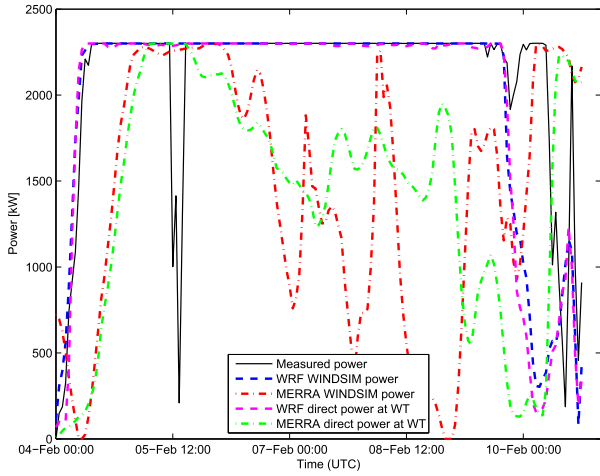
Table 1 (Dir. = Direct at wind turbine, WIND. = WindSim) summarized the RMSE values for all of the applied methods with respect to measured values at the wind turbine. WRF-WindSim coupling preformed better compared to MERRA-WindSim coupling in all three test cases, as RMSE decreased by 70.9% for the February case, 61.5% for October and 14.4% for June case respectively. Mesoscale winds from the WRF model are closer to the measurements than the mesoscale winds taken from the MERRA data set when extracted directly at the wind turbine, as shown by the decrease of the RMSE by 62.6% for the February case, 62.7% for October and 23.7% for June case respectively. It is evident that the output of the coupled model is influenced by the quality of input mesoscale winds. The mesoscale winds generated from WRF has the suitable boundary conditions along with appropriate set of physical configurations. MERRA dataset generally succeeded in capturing the overall shape of the wind profile but is largely underestimated. Both WRF and MERRA give the mesoscale winds as grid points. The values at the grid point actually represent an area average over a grid box. In current WRF model, one grid value represent an area average over  $2 \text{ km} \times 2 \text{ km}$  whereas in MERRA dataset one grid value represent an area average of  $27 \text{ km} \times 57 \text{ km}$ , at this site. Undoubtedly, MERRA values are more prone to have errors as compared to WRF due to neglecting the terrain variations over large distances. Another potential error comes from interpolating to turbine location from the grid values. This interpolation is required to compare the model values with measured values recorded at the turbine location. WRF grid point are 2 km apart whereas MERRA grid points are much farther and hence have higher vulnerability to interpolation errors. However, these interpolation errors are not expected to be as large as the inherit sources of errors that weather models have in general resulting from e.g. initial and boundary conditions, domains sizes, vertical and horizontal resolution, terrain resolution, vegetation characteristics, nudging and data assimilation. The difference between WRF-WindSim vs MERRA-WindSim and WRF direct vs MERRA direct RMSE results are significant when using *t*-test with 5% confidence interval for all three high wind events.

### 5.2. Wind power analysis

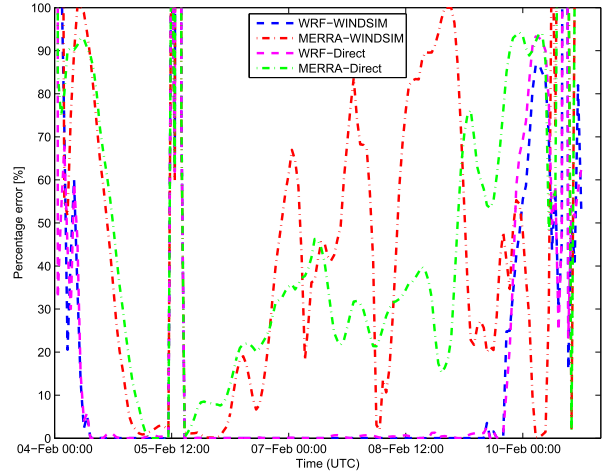
Figs. 6 and 7 show the result of power outputs and corresponding percentage errors from the two coupled models. Fig. 6 shows that WRF direct and WRF-WindSim was successful in following the power output trend in cases (a) and (b). Only exception is the dip in power estimation at the end of case (a), which is understandable since it corresponding from the dip in wind speed prediction in same case. The spike showing sudden loss of measured power around the beginning in case (a) is most probably a measurement error. MERRA direct and MERRA-

Table 1  
RMSE with respect to measured data.

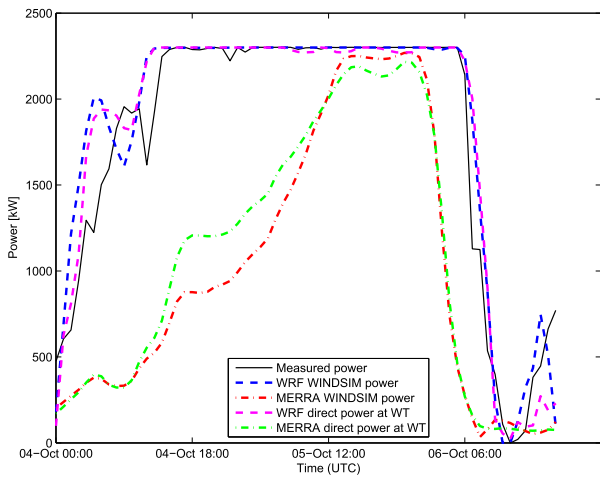
	WRF Dir.	WRF-WIND.	MERRA Dir.	MERRA-WIND.
February	2.86	2.38	7.65	8.20
October	1.76	1.90	4.72	4.94
June	4.61	5.21	6.04	6.09



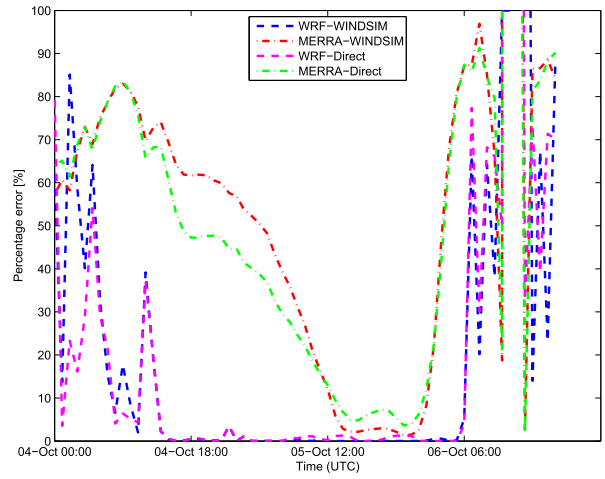
(a) Case: February 4-10 2009



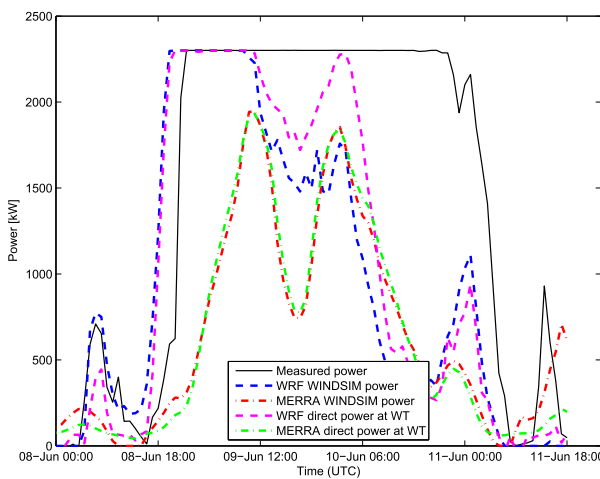
(a) Case: February 4-10 2009



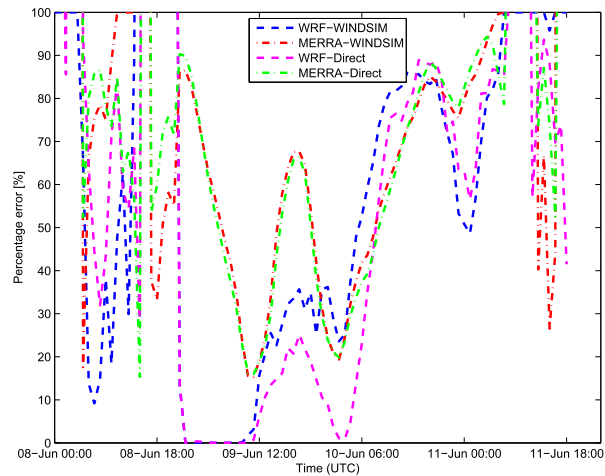
(b) Case: October 4-6 2008



(b) Case: October 4-6 2008



(c) Case: June 8-11 2008



(c) Case: June 8-11 2008

Fig. 6. Comparison of WRF, MERRA WindSim-Direct power output vs measured values.

Fig. 7. Percentage errors of WRF, MERRA WindSim-Direct power output vs measured values.

WindSim showed underestimation and randomness while following the measured power trend in all the three cases. The same pattern is translated to Fig. 7, showing the percentage errors with respect to measured power.

## 6. Conclusion

The results suggest that the performance of microscale model is largely dependent upon the quality of input mesoscale winds used as virtual climatology. In terms of using WindSim, further testing is recommended on the sensitivity of the initial boundary conditions to the accuracy of the converged solution. That includes testing of different wind speeds at the inlet, but also testing different boundary layer height as a too low value might result in artificial blocking and speed up. Conducting tests with finer wind direction sectors is recommended for future cases. The wind direction width for the current project was 30°. By increasing the number of wind direction sectors, influence of local terrain could be captured with higher accuracy and that might improved the wind speed predictions.

When comparing the results at the wind turbine location between direct mesoscale winds and the output of coupled model, WindSim could not capture the complex terrain and the corresponding inflow angles as good as expected. Although WindSim has a resolution of 20 m × 20 m, one possible reason could be the mismatch between grid sizes of WRF, MERRA and WindSim in this study. The coupled WRF-WindSim model takes a WRF wind speed which is an average value over 2 km × 2 km grid box and uses this value as wind speed input in WindSim as constant value for several 20 m × 20 m grid boxes. This is a change in terrain of approximately 100 times without any change in wind speed. In case of MERRA dataset, the transformation is even bigger. The meso-microscale based WRF-WindSim coupling model showed a better solution for predicting the wind behaviour over the complex terrain of Nygårdsfjell than the MERRA-WindSim coupling. Further testing of the proposed technique on larger datasets is recommended. For preliminary wind resource and seasonal variations assessment, WRF can be used for acceptable results. WRF and WindSim work in a complementary manner, whereby WRF solves the general wind fields by taking into account the physical processes and atmospheric conditions, while WindSim calculates the terrain induced local speed-up effects.

## Acknowledgement

Gratitude is extended to Nordkraft Vind for granting access to their data. The project is fully funded by the Arctic University of Norway.

## References

[1] J. Nossent, P. Elsen, W. Bauwens, Sobolsensitivity analysis of a complex

environmental model, *Environ. Model. Softw.* 26 (12) (2011) 1515–1525.

[2] J. R. Krieger, J. Zhang, D. E. Atkinson, X. Zhang, M. D. Shulski, P1. 2 sensitivity of wrf model forecasts to different physical parameterizations in the beaufort sea region.

[3] S. Hirabayashi, C.N. Kroll, D.J. Nowak, Component-based development and sensitivity analyses of an air pollutant dry deposition model, *Environ. Model. Softw.* 26 (6) (2011) 804–816.

[4] M.J. Barnsley, *Environmental Modeling: a Practical Introduction*, CRC Press, 2007.

[5] I. Orlanski, A rational subdivision of scales for atmospheric processes, *Bull. Amer. Meteor. Soc.* 56 (5) (1975) 527–534.

[6] N.K. Awan, H. Truhetz, A. Gobiet, Parameterization-induced error characteristics of mm5 and wrf operated in climate mode over the alpine region: an ensemble-based analysis, *J. Clim.* 24 (12) (2011) 3107–3123.

[7] V. Kapos, J. Rhind, M. Edwards, M. Price, C. Ravilious, N. Butt, et al., Developing a map of the world's mountain forests., *Forests in sustainable mountain development: a state of knowledge report for 2000*, Task Force For. Sustain. Mt. Dev. (2000) 4–19.

[8] S.V. Kumar, C.D. Peters-Lidard, J.L. Eastman, W.-K. Tao, An integrated high-resolution hydrometeorological modeling testbed using lis and wrf, *Environ. Model. Softw.* 23 (2) (2008) 169–181.

[9] D. Carvalho, A. Rocha, M. Gómez-Gesteira, C. Santos, A sensitivity study of the wrf model in wind simulation for an area of high wind energy, *Environ. Model. Softw.* 33 (2012) 23–34.

[10] M. Bilal, Y. Birkelund, M. Homola, High winds at nygårdsfjell, *J. Clean Energy Technol.* 3 (2) (2015) 106–109.

[11] J.A. Carta, S. Velázquez, P. Cabrera, A review of measure-correlate-predict (mcp) methods used to estimate long-term wind characteristics at a target site, *Renew. Sustain. Energy Rev.* 27 (2013) 362–400.

[12] M. Kubik, D.J. Brayshaw, P.J. Coker, J.F. Barlow, Exploring the role of reanalysis data in simulating regional wind generation variability over northern Ireland, *Renew. Energy* 57 (2013) 558–561.

[13] I. Staffell, R. Green, How does wind farm performance decline with age? *Renew. Energy* 66 (2014) 775–786.

[14] U.B. Gunturu, C.A. Schlosser, Characterization of wind power resource in the United States, *Atmos. Chem. Phys.* 12 (20) (2012) 9687–9702.

[15] M.M. Rienecker, M.J. Suarez, R. Gelaro, R. Todling, J. Bacmeister, E. Liu, M.G. Bosilovich, S.D. Schubert, L. Takacs, G.-K. Kim, et al., Merra: Nasa's modern-era retrospective analysis for research and applications, *J. Clim.* 24 (14) (2011) 3624–3648.

[16] M. J. Suarez, M. Rienecker, R. Todling, J. Bacmeister, L. Takacs, H. Liu, W. Gu, M. Sienkiewicz, R. Koster, R. Gelaro, et al., The geos-5 data assimilation system—documentation of versions 5.0. 1, 5.1. 0, and 5.2. 0.

[17] H.H. Shin, S.-Y. Hong, Intercomparison of planetary boundary-layer parameterizations in the wrf model for a single day from cases-99, *Bound. Layer Meteorol.* 139 (2) (2011) 261–281.

[18] A. Balzarini, F. Angelini, L. Ferrero, M. Moscatelli, M. Perrone, G. Pirovano, G. Riva, G. Sangiorgi, A. Toppetti, G. Gobbi, et al., Sensitivity analysis of pbl schemes by comparing wrf model and experimental data, *Geosci. Model Dev. Discuss.* 7 (5) (2014) 6133–6171.

[19] X.-M. Hu, J.W. Nielsen-Gammon, F. Zhang, Evaluation of three planetary boundary layer schemes in the wrf model, *J. Appl. Meteorol. Climatol.* 49 (9) (2010) 1831–1844.

[20] E. Berge, A.R. Gravidahl, J. Schelling, L. Tallhaug, O. Undheim, Wind in complex terrain. A comparison of WASP and two CFD-models, *Proc. EWEC* 27 (2006).

[21] T. Wallbank, *Windsim Validation Study*, CFD Validation in Complex Terrain, 2008.

[22] D.I.C. Albrecht, M. Klesitz, Three-dimensional wind field calculation above orographic complex terrain in southern Europe, in: *European Wind Energy Conference*, Athens, 2006.

[23] J. Gallagher, *An Assessment of the Discrepancy between Operational Assessment and Wind Resource Assessment for a Wind Farm in Ireland*, 2014.

[24] D. Papanastasiou, D. Melas, I. Lissaridis, Study of wind field under sea breeze conditions; an application of wrf model, *Atmos. Res.* 98 (1) (2010) 102–117.